Proceedings of DETC'97
1997 ASME Design Engineering Technical Conferences
September 14-17, 1997, Sacramento, California

DETC97VIB-3907

ANALYTICAL AND EXPERIMENTAL INVESTIGATION OF AN IMPACT OSCILLATOR

M. Oestreich, N. Hinrichs, K. Popp
Institute of Mechanics
University of Hannover
30167 Hannover, Germany
Email: oest@ifm.uni-hannover.de

C. J. Budd
School of Mathematics
University of Bath
Bath, U. K.
Email: cjb@math.bath.ac.uk

ABSTRACT

In the present paper a single-degree-of-freedom, periodically forced impact oscillator is investigated by numerics and experiments. At first the different types of motion and bifurcation diagrams are determined from experiments and compared to numerical results on the basis of the identified impact model. Also the nonsmooth third order system shows a rich bifurcational behaviour. On the basis of the identified nonsmooth model further analytical and numerical analysis can be applied. The Lyapunov exponents and the winding number are evaluated for the nonsmooth system.

INTRODUCTION

During the past decade nonsmooth dynamical systems have become increasingly important in engineering and other applied sciences as nonsmooth effects are genuinely taken into account and are no longer smoothed out. The nonsmooth system investigated here is a driven impact oscillator, in which the components undergo instantaneous, discontinuous, changes of motion due to impacts. Such systems or related systems with piecewise linear restoring forces arise naturally in many applications. Fig. 1 shows some examples, for example the sound of a church bell (Fig. 1(a)). Other Examples arising in mechanical engineering applications include rattling gear boxes (Kaharaman and Singh [1990], Prestl [1990]), (Fig. 1(b)) and impact print hammers (Tung and Shaw [1988]), (Fig. 1(c)). In these latter two examples, problems in the mechanism arise from the noise and wear associated with successive impacts. Similar wear problems arise in boiler tubes and in nuclear reactor fuel rods. Impact also plays a role in biological systems including studies of walking (McGeer [1990]) and in DC-DC buck convertors (diBernardo et al. [1996]) where the action of pulse width modulation of the supply is very similar to an impacting process. Early studies of impact oscilla-

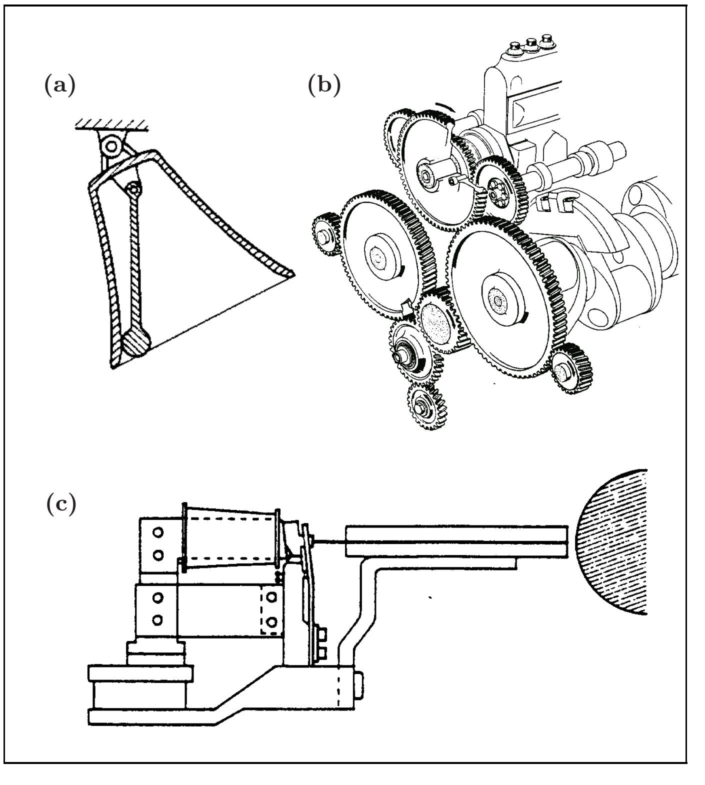

Figure 1. EXAMPLES FOR SYSTEMS WITH IMPACTS.

tors comprised numerical investigations by Peterka et al. [1974a, 1974b] whereas in more recent studies initiated by Shaw and Holmes [1983], Whiston [1987], Foale and Bishop [1992], Nordmark [1991], Budd et al. [1994a, 1994b, 1995a, 1995b, 1995c, 1996a, 1996b], Chin et al. [1994], ideas from the modern theory of dynamical systems have been applied to both explain existing results and predict new and complex behaviour. Some experimental investigations of the impact oscillator have been done by Stensson and Nordmark [1994] who investigated an impacting pendulum, by Foale and Bishop [1992] who investigated an impacting cantilever beam and by Hinrichs et al. [1997] who looked at the impacts of a rigid bar. The theoretical investigations have revealed a richness of dynamics much of which is novel and associated with the essential discontinuous nature of impacting dynamics. In particular, several new forms of bifurcation including the *grazing bifurcation* (Nordmark [1991]) have been identified as new routes to chaos. The experimental work has demonstrated that much of this richness is also observed in practical demonstrations - with much still unexplained behaviour. It is clear that the great variety of the dynamics observed in impact oscillators continues to provide fascinating challenge for both theoretical and experimental work.

In this paper we perform two comparisons between experimental and analytical investigations. Firstly, we report on some results of some careful experiments with a rigid beam impacting an obstacle and show that many of the complex dynamical phenomena predicted from the theory are observed in practice. Earlier experiments have in general not revealed some of these phenomena and have shown less satisfactory aggreement with theoretical predictions. Then we compare two maps associated with the impact map - relating the stroboscopic map which is the natural tool of the experimentalist with the impact map which is the natural tool for analysis. In particular, by focusing attention on the Lyapunov exponents of the system, we establish a relation between the action of the two maps via the associated winding number of the oscillator.

INVESTIGATED SYSTEM

One of the simplest impact oscillators which can be studied both analytically and experimentally comprises a periodically forced mass m at a position $x(t)$ acting as a harmonic oscillator with an instantaneous impact against a fixed stop in which the velocity is reversed and reduced by a factor r. Although this model appears to be very simple, the close correspondence between experimental and theoretical results gives support to its credibility. In this section we give both a theoretical model of this and an experimental realisation.

Mechanical model

The mechanical model used for the impact oscillator is shown in Fig. 2. To model this system we consider the mass to be subject to a restoring force due to a linear spring of stiffness c and to linear damping b. The location of $x(t)$ is everywhere constrained to be greater than σ where σ is the location of a rigid stop. The whole system is given an external excitation $u(t) = u_0 \cos \Omega t$ and we define the ratio of Ω to the natural frequency ω_0 of the unforced system by η. If $x = \sigma$ the mass impacts with the stop and its velocity is reversed and its absolute value is reduced by the factor r. The equation of motion for such a system then becomes

$$\begin{aligned} m\ddot{x}(t) + b\dot{x} + cx(t) &= cu_0 \cos \Omega t, \quad \text{for} \quad x > \sigma, \\ \dot{x}(t^+_{imp}) &= -r\dot{x}(t^-_{imp}), \quad \text{for} \quad x = \sigma, \end{aligned} \tag{1}$$

where t_{imp} is the (instantaneous) time of an impact, $\dot{x}(t^+_{imp})$ is the velocity immediately after the impact and $\dot{x}(t^-_{imp})$ is the velocity immediately before the impact. To describe the behaviour at the impact we apply Newton's law of restitution where the velocity of the mass reverses at each impact with $r \leq 1$ as the coefficient of restitution. This rough simplification assumes vanishing impact time and infinite contact forces for the rigid stop.

The equation of motion can be normalized using

$$\tau = \omega_0 t, \;\; \omega_0 = \sqrt{\frac{c}{m}}, \;\; \eta = \frac{\Omega}{\omega_0}, \;\; (*)' \equiv \frac{d(*)}{d\tau} = \frac{(\dot{*})}{\omega_0}. \tag{2}$$

From eqs. (1) and (2) it follows

$$\begin{aligned} x''(\tau) + 2Dx(\tau) + x(\tau) &= u_0 \cos \eta\tau, \quad \text{for} \;\; x > \sigma, \\ x'(\tau^+_{imp}) &= -rx'(\tau^-_{imp}), \;\; \text{for} \;\; x = \sigma. \end{aligned} \tag{3}$$

where the normalised damping coefficient D is given by $D =$

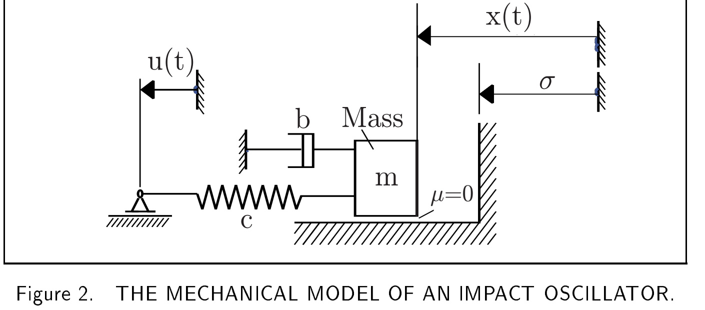

Figure 2. THE MECHANICAL MODEL OF AN IMPACT OSCILLATOR.

$\frac{b}{2\sqrt{cm}}$. Defining the state vector $\mathbf{z} = [z_1, z_2, z_3]^T = [x, v, \tau]^T$ the corresponding system of autonomous differential equations for $x > \sigma$ becomes

$$\begin{aligned} z_1' &= z_2, \\ z_2' &= -2Dz_2 - z_1 + u_0 \cos \eta z_3, \\ z_3' &= 1, \end{aligned} \tag{4}$$

where $v = x'(\tau)$ is the velocity of the mass.

In general a motion of the mass comprises a recurrent series of impacts with the stop separated by a smooth evolution between impacts. Owing to energy loss both at impacts and between impacts, such motion is dissipative and asymptotically evolves toward either a periodic motion or a chaotic motion on a strange attractor. As parameters in the model are varied we observe changes in stability of these asymptotic states with transitions between them described by either smooth (period doubling or saddle-node) bifurcations or by non-smooth grazing bifurcations. It is also possible to have motion which ultimately does not impact with the stop at all. This behaviour is linear and will not be considered it further in this paper.

Experimental setup

The experimental investigation of the impact oscillator uses the test stand illustrated in Fig. 3(a) . Here the linear oscillator is represented by a stiff beam 1 which rotates about a bearing in one plane with a restoring force provided by two linear springs 2. By using air bearings 3 the motion takes place with a very small damping coefficient $D < 0.005$. The beam is carefully constrained by the bearing to move in one plane only. The harmonic excitation is realized by means of a controlled electromagnetic force generated at the end of one arm of the beam (Fig. 3(b)). The parameter of the force excitation can be slowly varied to sweep through a bifurcation diagram. An impact takes place if the beam hits a spherical obstacle 4 made of aluminium (Fig. 3(c)). The velocity of the beam is measured directly by a laser-Doppler vibrometer and its position obtained by integrating this measurement. A more extended description of the test stand is given in Hinrichs et al. [1997b]. The experiment is precisely described by the model in the previous section and accordingly we may determine the associated system parameters. For our setup these are $m = 0.091kg$, $b = 0.017kg/s$, $c = 88.371N/m$, $u_0 = 0.004m$. The coefficient of restitution r is measured by examining the velocity change at impact in the absence of forcing over several impacts and for the experiments reported in this paper is found to be $r = 0.86$.

In contrast with other experimental investigations of the impact oscillator using pendulums or cantilever beams, the rigidity of the metal beam and its constrained motion in one plane only, ensures that the motion is truly one-dimensional and also the motion is primarity in the dominant vibrational mode determined by the spring constants. Although a small component of a higher harmonic mode (due to vibrations of the body of the beam) is generated at each impact, its effect is minor and is very rapidly damped out. In contrast, the cantilever beam loses a significant amount of energy at each impact to the higher modes. As the contribution of the higher modes is so small the system (2) is a good representation of the dynamics of this particular experiment and the assumption of an instantaneous impact is reasonable.

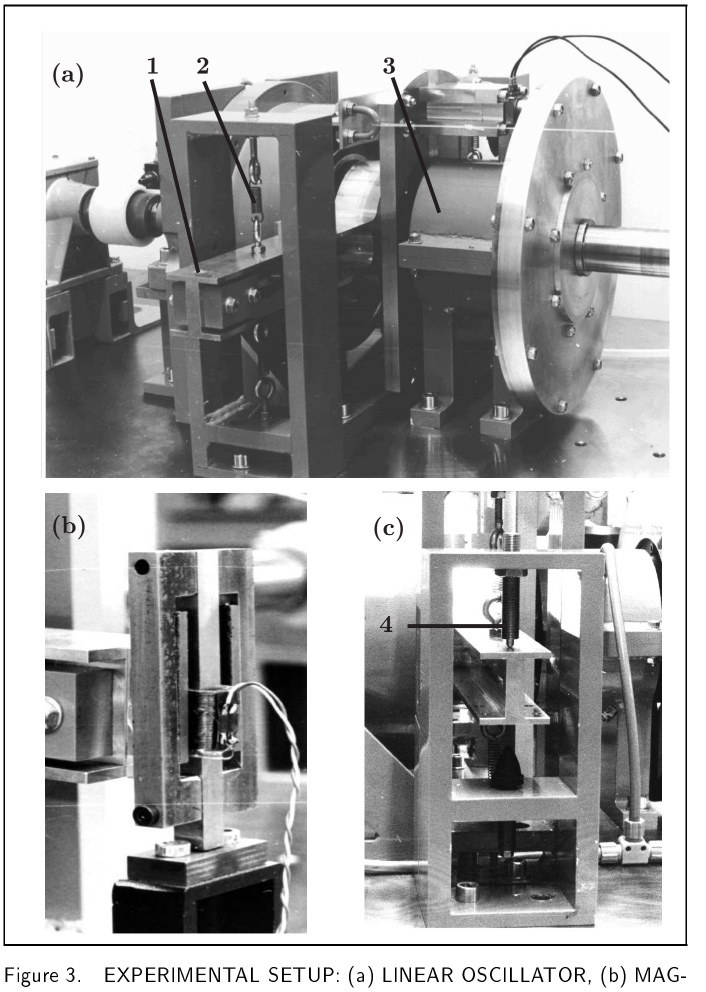

Figure 3. EXPERIMENTAL SETUP: (a) LINEAR OSCILLATOR, (b) MAGNETIC EXCITATION, (c) IMPACT AT STOP.

NUMERICAL AND EXPERIMENTAL RESULTS

The results from the experiments can be compared with numerical experiments using (2) and the identified system parameters. Figure 4 shows different types of experimentally measured phase trajectories, where the velocity v of the beam is shown as a function of the displacement x. In the plots the displacement x is scaled in [mm] and the velocity v in [mm/s]. For $\eta = 3.0$ the motion repeats periodically after two impacts(Fig. 4(a)) and two forcing periods. For $\eta = 2.76$ the motion repeats after three impacts and two forcing periods (Fig. 4(b)) and for $\eta = 2.9$ the motion is apparantly chaotic (Fig. 4(c)). We refer to the first two forms of periodic motion as (2,2) and (3,2) orbits respectively. From these figures the effect of the higher modes of oscillation can be seen clearly in the motion of the beam immediately after the impact.

For the system equation (3) or (4) the trajectory can also be simulated and investigated analytically. (Details of the techniques for this calculation are given for example in Budd et al. [1995c]). In particular, for the values of η given it is found that (2,2) orbits, (3,2) orbits and chaotic motions exist. The results of the simulations are presented in (Fig. 5) on the basis of the identified setup parameters, and show a good agreement with the experimental ones. Due to the simple model for the impact supposing zero impact time and rigid contact bodies the trajectories differ during the impact and immediately after the impact but in the periodic case the period of the solution is predicted accurately and in all three cases the amplitude is also predicted accurately by the simulations.

The above calculations demonstrate periodic and chaotic motions, but some other motions peculiar to impacting oscillators have also been identified analytically and can also be seen in the experiments. A particularly interesting example of such behaviour is 'chatter' (Budd and Dux [1994a]), in which the pendulum repeatedly strikes the obstacle in a very short time interval before coming to rest and 'sticking' to it whilst the forcing is toward the obstacle and then being released when the forcing changes sign. An

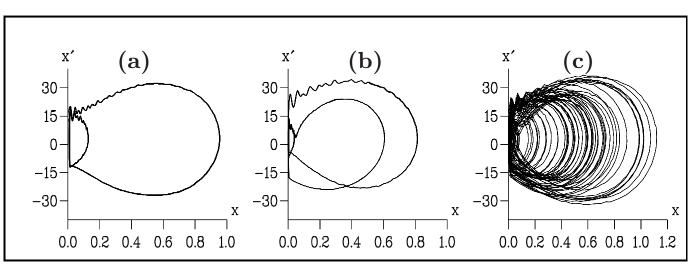

Figure 4. DIFFERENT TYPES OF MOTION: MEASUREMENTS FOR $\sigma = 0.0$, (a) $\eta = 3.0$, (b) $\eta = 2.76$, (c) $\eta = 2.9$.

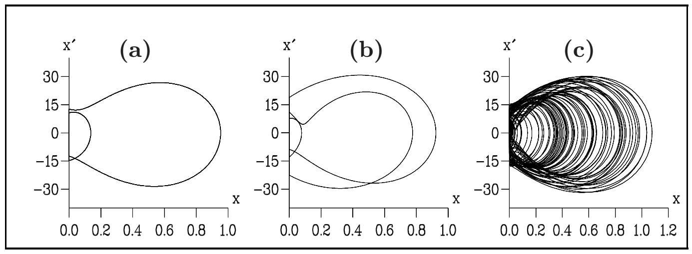

Figure 5. DIFFERENT TYPES OF MOTION: SIMULATIONS FOR $\sigma = 0.0$, (a) $\eta = 3.0$, (b) $\eta = 2.76$, (c) $\eta = 2.9$ (CP. WITH FIG. 4)

example of measured chatter is presented in Fig. 6(a), (b) in which the repeated impacts are clearly visible. A simulation at the same values of the identified parameters also predicts chattering behaviour which is comparable to the measured values.

A more global overview of the overall behaviour over a range of values of η can be obtained by slowly changing the value of η in the experiment, allowing the system to reach an asymptotic state (typically after more than 120 seconds) which is typically a periodic or a chaotic attractor, and then recording the next impacts (up to 20 seconds). In these calculations, the initial state of the system was taken to be at equilibrium with $x = v = 0$. A similar diagram can also be obtained by direct numerical simulation. To record the data a Poincaré section is taken so that the values of x are recorded when $v = 0$. The results from simulations and measurements are given in the two cases of $\eta < 2.5$ (Fig. 7(a),(b)) and $2 < \eta < 4$ (Fig. 8(a),(b)). Several features of the simulated and measured bifurcation diagrams agree very well. In particular, large resonant peaks can be seen for the even values of $\eta = 2n$ at which the motion is periodic and repeats after one impact and n forcing periods. In contrast as $\eta \to 3$ the amplitude of the oscillation decreases and there is a period-doubling bifurcation to a (2,2) orbit at $\eta \approx 2.6$ visible in both pictures. For slightly greater values of η a (3,2) periodic motion occurs following a grazing

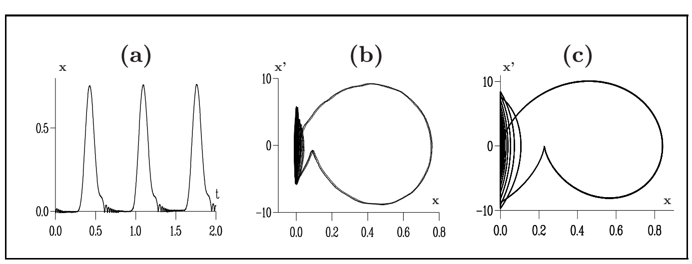

Figure 6. MOTION WITH CHATTER: MEASUREMENTS FOR $D = 0.004$, $u_0 = 0.0023$, $r = 0.87$, $\eta = 0.3$, $\sigma = 0.0$, (a) MEASURED TIME HISTORY OF THE DISPLACEMENT x, (b) MEASURED PHASE TRAJECTORY, (c) SIMULATED PHASE TRAJECTORY.

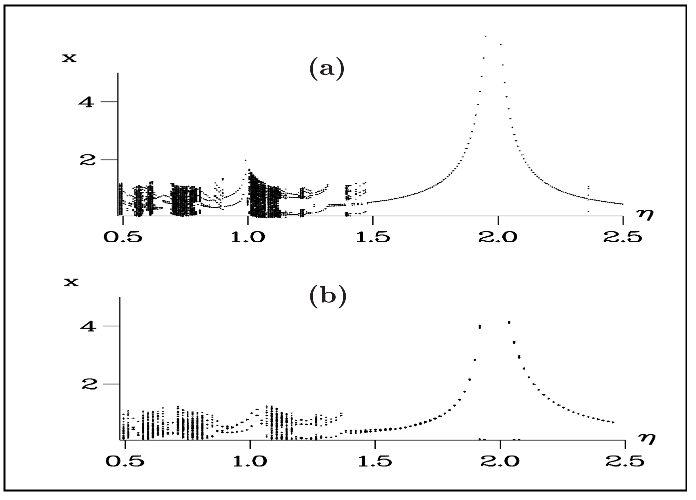

Figure 7. BIFURCATION DIAGRAM SHOWING (a) SIMULATION AND (b) MEASUREMENT: $D = 0.004$, $u_0 = 0.0023$, $r = 0.92$, $\sigma = 0.0$.

bifurcation which is then followed by a region of chaotic motion. Around $\eta = 3$ there is an interval of (2,2) motion which agrees with the analytic predictions made in Budd and Lee [1996b]. (This motion is in fact a restabilisation of the 2-periodic motion created in the period-doubling bifurcation). For larger values of η there is a small chaotic window before the creation of a stable (1,2) periodic orbit which evolves toward the resonant peak at $\eta = 4$. There are some differences between experiment and theory. In particular, the interval of existence of the (2,2) orbits centered on $\eta = 3$ appears larger in the experiment than in the simulation. Furthermore, in the simulated bifurcation diagram there is a chaotic region at $\eta = 2.7$, which cannot

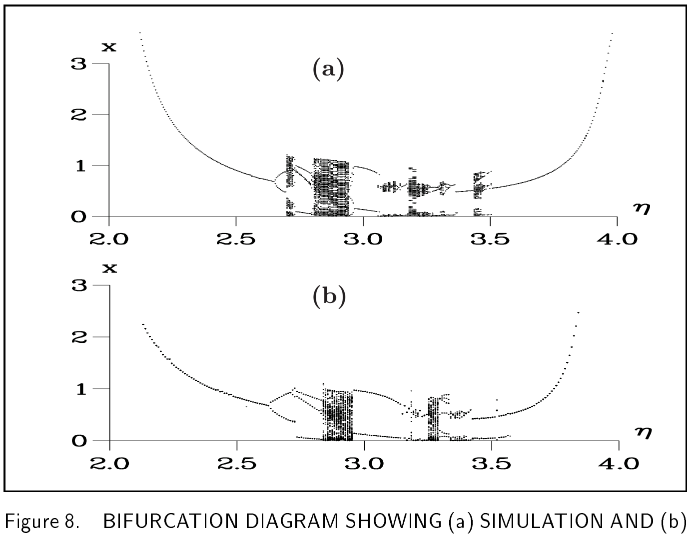

Figure 8. BIFURCATION DIAGRAM SHOWING (a) SIMULATION AND (b) MEASUREMENT: $D = 0.006$, $u_0 = 0.0043$, $r = 0.86$, $\sigma = 0.0$.

be found in the measurements. In this region the theory predicts that there are coexisting solutions which depend upon the initial conditions, and these are not recorded in the measurements. Further bifurcation diagrams for simulations and measurements can be found in Hinrichs et al. [1997a].

THEORETICAL ANALYSIS OF THE SYSTEM BEHAVIOUR

As the impact oscillator has been studied analytically in several papers (see the references given in this paper) we only review the theory very briefly here. Our main interest is to compare two different approaches for measuring and analysing the behaviour of the oscillator.

Poincaré maps

The impact oscillator can be studied by the use of two independent (though related) Poincaré maps termed the Stroboscopic and Impact maps respectively, which are respectively convenient for experimental and analytic investigations. In practice, experimental measurements, particularly with the laser Doppler methods described will be made at equally spaced time intervals as the velocity of the beam is sampled at a fixed rate. Observing (see Budd et al. [1995c]) that all periodic motions of the system have a period which is a multiple of the forcing period $T = \frac{2\pi}{\omega}$ we see that a convenient map is given by

$$P_S(x(t), v(t)) = (x(t+T), v(t+T)) \tag{5}$$

This map acts on the phase space $(\sigma, \infty) \times (-\infty, \infty)$ of possible positions and velocities (x, v) of the mass at the sample times and is always defined for quite general data in this space. For a particular trajectory $\mathbf{z}(t)$ of the extended system (x, v, τ) defined in section 2.1 the map P_S corresponds to the points of intersection of $\mathbf{z}(t)$ with the planes $[x, v, \tau]$ with $\tau = nT, n = 0, 1, 2, ...$ Observe that not all of the possible initial data for this map actually leads to impacting motions.

A disadvantage of using the stroboscopic map for analysis is that in general it is unknown how many impacts there will be between two sampling periods. Given that it is the impacts which essentially govern the dynamics of the oscillator, this problem makes it difficult to deduce the dynamical behaviour of the oscillator from P_S alone.

To overcome this, for the purposes of analysis it is preferable to use the impact map P_I which relates the conditions at one impact to the next and focuses attention on the critical role played in the dynamics by the impacts themselves. The construction of this map relies upon the important observation that if there is no energy loss between impacts (i.e. if the damping coefficient $D = 0$) then impacting motion is recurrent. Thus, if an impact occurs at a time τ_i then there will be a subsequent time τ_{i+1} at which there will be a next impact. For the remainder of this paper we make this assumption on D. Observe from the experimental work that D is very small owing to the use of the air bearing. Suppose now that an impact with the stop at $x = \sigma$ occurs with negative velocity v_i at the time τ_{i+1}. The effect of the impact is to change the velocity to $-rv_i$. The system then evolves forward in time before striking the stop at first time $\tau_{i+1} > \tau_i$ with negative velocity v_{i+1}.

We then define P_I by

$$P_I(v_i, \tau_i) = (v_{i+1}, \tau_{i+1}).$$

As the underlying system has a periodic excitation of period T. It is generally more convenient to identify a phase

$$\phi_i = (\tau_i)_T$$

and then to consider P_I as a map from (v_i, ϕ_i) to (v_{i+1}, ϕ_{i+1}), so that P_I acts on the cylindrical phase space $(v, \phi) \in (-\infty, 0] \times [0, T]$, where $\phi = 0$ is identically to $\phi = T$.

For the same trajectory $\mathbf{z}(t)$ considered above, the iterates of P_I correspond to the intersections of $\mathbf{z}(t)$ with the plane $x = \sigma$ with $v < 0$.

The impact map can be constructed explicitly by decomposing the motion of the beam into an impacting phase and a free flight phase.

In the impacting phase we have

$$(v_i, \phi_i) \to (-rv_i, \phi_i).$$

In the free flight phase, the motion is described by the solution of a forced harmonic oscillator with initial conditions $x = \sigma, v = -rv_i, \tau = \phi_i$ and can be solved exactly to give

$$\begin{aligned} x(\tau) = {} & \frac{u_0}{1-\eta^2}\cos(\eta\tau) \\ & + C_1\cos(\tau - \phi_i) + C_2\sin(\tau - \phi_i), \end{aligned} \tag{6}$$

$$\begin{aligned} v(\tau) = {} & -\frac{\eta u_0}{1-\eta^2}\sin(\eta\tau) \\ & - C_1\sin(\tau - \phi_i) + C_2\cos(\tau - \phi_i), \end{aligned} \tag{7}$$

where $C_1 = \sigma - \frac{1}{1-\eta^2}\cos(\eta\phi_i)$ and $C_2 = -rv_i + \eta\frac{1}{1-\eta^2}\sin(\eta\phi_i)$.

This solution (6) is valid for $\phi_i \leq \tau < \tau_{i+1}$ where τ_{i+1} with associated phase ϕ_{i+1} is the time of the next impact given by the first solution of the transcendental equation $x(\tau) - \sigma = 0$. Whilst a closed form of P_I cannot be given explicitly it can be evaluated numerically. Furthermore, implicit differentiation gives an expression for the Jacobian derivative DP_I via the relations

$$\begin{aligned} \frac{\partial \phi_{i+1}}{\partial \phi_i} &= -\frac{1}{v_{i+1}}\frac{\partial x}{\partial \phi_i}\bigg|_{\tau=\tau_{i+1}}, \\ \frac{\partial \phi_{i+1}}{\partial v_i} &= -\frac{1}{v_{i+1}}\frac{\partial x}{\partial v_i}\bigg|_{\tau=\tau_{i+1}}, \\ \frac{\partial v_{i+1}}{\partial \phi_i} &= \frac{\partial v}{\partial \phi_i}\bigg|_{\tau=\tau_{i+1}} + x''|_{x=\sigma}\frac{\partial \phi_{i+1}}{\partial \phi_i}, \\ \frac{\partial v_{i+1}}{\partial v_i} &= \frac{\partial v}{\partial v_i}\bigg|_{\tau=\tau_{i+1}} + x''|_{x=\sigma}\frac{\partial \tau_{i+1}}{\partial v_i}. \end{aligned} \tag{8}$$

Thus

$$DP_I = \begin{bmatrix} \frac{1}{v_{i+1}}(-rv_i c_{10} + A_0 s_{10}) & -\frac{r}{v_{i+1}}s_{10} \\ -B_1 c_{10} - B_2 s_{10} & -r\left(c_{10} - \frac{A_1}{v_{i+1}}s_{10}\right) \end{bmatrix} \tag{9}$$

where $B_1 = A_0 + rA_1\frac{v_i}{v_{i+1}}$, $B_2 = rv_i - \frac{A_0 A_1}{v_{i+1}}$, $s_{10} = \sin(\tau_{i+1} - \tau_i)$, $c_{10} = \cos(\tau_{i+1} - \tau_i)$, and $A_0 = \cos(\eta\tau_i) - \sigma$, $A_1 = \cos(\eta\tau_{i+1}) - \sigma$ are the accelerations at the two impacts. Thus DP_I is defined uniquely by equation (9). It follows immediately that the determinant of DP_I is

$$\det(DP_I) = r^2\frac{v_i}{v_{i+1}}. \tag{10}$$

Observe that if v_{i+1} is small then P_I can locally introduce a great deal of stretching into the phase plane. This phenomena is associated with grazing and the related grazing bifurcation reported in Chin et al. [1994] and leads directly to much of the rich behaviour observed in impacting dynamics.

A comparison of stroboscopic and impact maps

We now look at the relation between the two maps constructed in the previous section. The simplest comparison is afforded by looking at a (m,n) periodic trajectory $\mathbf{z}(t)$ repeating after m impacts and n forcing periods. Such an orbit is a fixed point of P_I^m and of P_S^n. For an orbit which includes chatter we can have $m = \infty$ and n finite. Converseley, it is shown in Budd et al. [1995c] that periodic orbits can exist with $m = 1$ and n taking arbitrarily large values. Thus the periodic orbits can look very different when expressed in terms of the two maps. However we can determine a very precise relationship between the actions of the two maps on their respective phase spaces.

To do this, we consider a trajectory $\mathbf{z}(t)$ which impacts recurrently such that any trajectory in a neighbourhood of $\mathbf{z}(t)$ also impacts recurrently. Suppose now that at $\tau = 0$ we have that the position and velocity of $\mathbf{z}(t)$ are given by $x(0) = x_\alpha$ and $v(0) = v_\alpha$. After the time interval T let $(x(T), v(T) = x_\beta, v_\beta$ so that $P_S(x_\alpha, v_\alpha) = (x_\beta, v_\beta)$. Now suppose that we consider an open set of data Ω_α of positions and velocities at time $\tau = 0$ which lie in a neighbourhood of (x_α, v_α) and which are mapped by P_S onto a set Ω_β which is a neighbourhood of (x_β, v_β). Let the area of Ω_α be A_α and that of Ω_β be A_β. As we have assumed that $D = 0$, then if none of the trajectories starting from Ω_α impact the stop, as there is no energy loss between $\tau = 0$ and $\tau = T$, it follows immediately that $A_\alpha = A_\beta$. In general, however, the trajectory $\mathbf{z}(t)$ impacts M times with the stop in the time interval $[0, T]$. If we presume that none of these impacts has zero velocity, then provided that Ω_α is sufficiently small, all of the trajectories starting from Ω_α will also impact M times. We now claim that

$$A_\beta = r^{2M} A_\alpha. \tag{11}$$

To see this, we presume that the trajectory $\mathbf{z}(t)$ impacts the stop at $\tau = \tau_0$ with velocity $v = v_0 < 0$ and that the set of trajectories starting from Ω_α impacts the stop in a set of times and velocities which form a neighbourhood I_0 of the point (v_0, τ_0) in the velocity-time phase space such that the boundary of the set Ω_α is joined to the boundary of I_0 by a surface S comprising a set of trajectories. This situation is illustrated in Fig. 9. Let I_0 have area B_0. We claim that in the limit of a small region Ω_α we have

$$A_\alpha = |v_0| B_0. \tag{12}$$

This result relates the action of the maps P_S and P_I on their associated phase spaces. Observe that as $|v_0| \to 0$ we have $B_0 \to \infty$. To establish (12) this relation, consider the extended dynamical system satisfied by (x, v, τ) and let $\mathbf{f}$ be the vector tanjent to the trajectories so that

$$\mathbf{f} = (v, -x + u_0 \cos \eta\tau, 1)^T.$$

It is immediate that $\nabla \mathbf{f} = 0$ and that $\mathbf{f}$ is everywhere tanjent to S. Consequently, the flux of $\mathbf{f}$ through the surface Ω_α

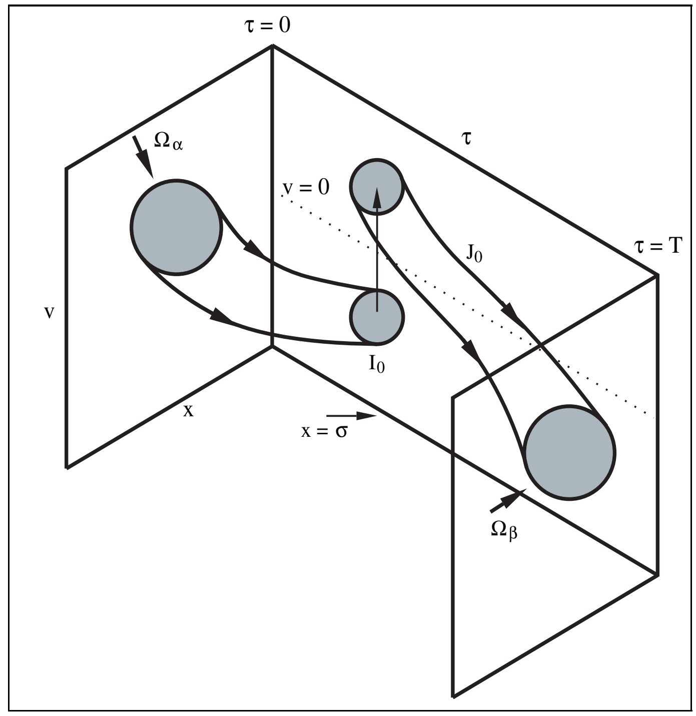

Figure 9. FLOW OF A SET OF TRAJECTORIES.

must equal that through the surface I_0 giving

$$|\int_{\Omega_\alpha} \mathbf{fn} d\Omega| = |\int_{I_0} \mathbf{fn} d\Omega|$$

where $\mathbf{n}$ is the normal and $d\Omega$ the area element. Now, on Ω_α we have τ fixed and hence $\mathbf{n} d\Omega = (0,0,1)^T dx dv$. Similarly on I_0 we have x is fixed and hence $\mathbf{n} d\Omega = (1,0,0)^T dv d\tau$. Thus

$$|\int_{\Omega_\alpha} dx dv| = |\int_{I_0} v dv d\tau|.$$

If I_0 is small then v is approximately equal to the constant v_0 so that $|\int_{I_0} v dv d\tau| \approx |v_0| B_0$. Furthermore $\int_{\Omega_\alpha} dx dv = A_\alpha$. In the limit of small I_0 this gives (12).

Now the set I_0 is mapped to a further set J_0 under the action of the impact so that points $(v, \tau) \in I_0$ are mapped to points $(-rv, \tau) \in J_0$. If the area of J_0 is C_0 then clearly

$$C_0 = r B_0$$

and C_0 is a neighbourhood of the point $(-rv_0, \tau_0)$.

Finally, suppose that the set J_0 is mapped onto the set Ω_β without any further impacts, then applying (12) to J_0

and Ω_β gives

$$A_\beta = r|v_0|C_0 = r^2|v_0|B_0 = r^2 A_\alpha.$$

Thus the action of one impact is to reduce the area of a set of data in the (x, v) space by a factor of r^2. Applying this argument succesively through M impacts gives the result (11) in the more general case.

We can generalise this argument to consider a series of iterations of the map P_S between the planes $\tau = iT, i = 0, \ldots, k$ taking the initial set Ω_α into the set Ω_γ with area A_γ. Suppose that between each iteration of the map we have $M_1, M_2, \ldots M_k$ impacts then

$$A_\gamma = r^{2(M_1+M_2+\ldots+M_k)} A_\alpha,$$

and hence the average rate of contraction in the phase space between each iteration of the map P_S is given by

$$\left(\frac{A_\gamma}{A_\alpha}\right)^{1/k} = r^{2\sum_{i=1}^{k}\frac{M_i}{k}} \to r^{2z} \quad \text{as} \quad k \to \infty \tag{13}$$

where

$$z = \lim_{k\to\infty}\left(\frac{1}{k}\sum_{i=1}^{k} M_i\right) \tag{14}$$

is the mean number of impacts per time interval T.

We define z to be the *winding number* of the flow. For an (m, n) periodic orbit, $z = m/n$ is rational. For a chaotic orbit, z is likely to be irrational.

A most interesting result occurs when chattering behaviour occurs and one of the terms M_i is infinite. In this case we have z infinite and the area of the corresponding set Ω_γ is zero. This result reflects super-stability properties of the chattering type orbits. Indeed, it is shown in Budd and Lee [1996b] that if an orbit is periodic and it has a chattering component, then all orbits within a neighbourhood of it are attracted onto it in a finite time interval.

The above arguments continue to hold in the case of a trajectory $\mathbf{z}(t)$ which impacts the obtacle with a velocity of zero provided that such impacts are not recurrent on the trajectory. In general this will be the case. We note, however, that close to a grazing bifurcation of the form described in Budd and Lee [1996b] there are chaotic orbits with reccurent low velocity impacts. These lead to interesting scaling properties of the related Lyapunov exponents as the bifurcation point is approached (Lambda and Budd [1994]).

Lyapunov exponents

An interesting application of the results of the last section appears in the computation of the Lyapunov exponents Λ_i for the impact oscillator. These measure the average rates of separation of the trajectories averaged over the attractor and give information on the rate of divergence of trajectories on a chaotic attractor, as well as the stability (or super stability) of periodic orbits. In practice (and for experimental purposes) these are computed from regular samples of the time series of the data so that if $\mathbf{z} \equiv (z_1, z_2, z_3) = (x, v, \tau)$ then the calculation of Lyapunov exponents is performed considering $\mathbf{z}$(t) as the solution in a 3-dimensional state space of the dynamical system $\mathbf{z}' = \mathbf{f}(\mathbf{z}(t))$, $\mathbf{z}(t_0) = \mathbf{z_0}$, $\mathbf{f} \in C^1$, with $\mathbf{f}$ as a continously differentiable vector function. A linearization of this equation yields

$$\delta\mathbf{z}' = \mathbf{F}(\tau)\delta\mathbf{z}(\tau), \quad \text{where} \quad \mathbf{F}(\tau) = \left.\frac{\partial \mathbf{f}(\mathbf{z})}{\partial \mathbf{z}^T}\right|_{z=z(\tau)} \tag{15}$$

denotes the Jacobian matrix of $\mathbf{f}$ with respect to the trajectory under consideration. In the smooth case the spectrum of the Lyapunov exponents Λ_i can be determined by

$$\lambda_i = \lim_{\tau\to\infty}\frac{1}{\tau}\ln\frac{||\delta\mathbf{z}(\tau)||}{||\delta\mathbf{z}_i(\tau_0)||} \tag{16}$$

for different initial conditions $\delta\mathbf{z_i}(\tau)$. This procedure cannot be applied directly to the nonsmooth impact oscillator as certain smoothness assumptions made in the underlying formulation are violated in this case. To overcome this we take care in the handling of the discontinuities in which the linearized equations are supplemented by transition conditions at the instants τ_i of the impacts (Müller [1995], Hubbuch et al. [1995]). An application of the determination of Lyapunov-exponents to another nonsmooth oscillator (friction oscillator) can be found in Oestreich et al. [1996a] and Hinrichs et al. [1997a].

For the nonsmooth impact oscillator the system equation (3) can be expressed as follows:

$$\begin{aligned}
(\tau_i \leq)\tau < \tau_{i+1}: \quad & \mathbf{z}' &&= \mathbf{f}(\mathbf{z}), \mathbf{z}(\tau_\mathbf{i}) = \mathbf{z_0}, \mathbf{f} \in C^1 \\
\tau = \tau_{i+1}: \quad & 0 &&= h(\mathbf{z}(\tau_{i+1})), h \in C^1 \\
& \mathbf{z}(\tau_{i+1}^+) &&= \mathbf{g}(\mathbf{z}(\tau_{i+1}^-)), \mathbf{g} \in C^1 \\
\tau_{i+2} > \tau > \tau_{i+1}: \quad & \mathbf{z} &&= \mathbf{f}(\mathbf{z}), \mathbf{z}(\tau_{i+1}) = \mathbf{z}(\tau_{i+1}^+)
\end{aligned}$$

with

$$\mathbf{f}(\mathbf{z}) = \begin{bmatrix} z_2 \\ -2Dz_2 - z_1 + u_0\cos(\eta z_3) \\ 1 \end{bmatrix}.$$

In each interval between between impacts, the system behaves smoothly with the same underlying function $\mathbf{f}$. The indicator function $h(\mathbf{z}) = z_1 - \sigma$ defines the instant of the impacts. The transition condition of the system at $\tau = \tau_{i+1}$ is given by the impact law, thus $\mathbf{g}(\mathbf{z}) = [z_1, -rz_2, z_3]^T$.
The linearized equation of motion before the impact reads:

$$\tau_i \le \tau < \tau_{i+1} : \delta\mathbf{z}' = \mathbf{F}(\tau)\delta\mathbf{z}, \ \ \delta\mathbf{z}(t_0) = \delta\mathbf{z}_0 \tag{17}$$

with

$$\mathbf{F}(\tau) = \begin{bmatrix} 0 & -1 & 0 \\ 1 & -2D & 0 \\ 0 & u_0\sin(\eta z_3) & 0 \end{bmatrix}.$$

The transition condition of the linearized equations at the impact yields

$$\begin{aligned} \delta\mathbf{z}_+ &= \mathbf{G}(\mathbf{z}_-)\delta\mathbf{z}_- \\ &\quad -[\mathbf{G}(\mathbf{z}_-)\mathbf{f}(\mathbf{z}_-) - \mathbf{f}(\mathbf{z}_+)]\frac{\mathbf{H}(\mathbf{z}_-)}{\mathbf{H}(\mathbf{z}_-)\mathbf{f}(\mathbf{z}_-)}\delta\mathbf{z}_- \end{aligned} \tag{18}$$

where

$$\mathbf{H}(\mathbf{z}_-) = \mathbf{H}(\mathbf{z}(\tau_{i+1}^-)) = \left.\frac{\partial h(z)}{\partial \mathbf{z}^T}\right|_{\mathbf{z}=\mathbf{z}(\tau_{i+1}^-)} = \begin{bmatrix} 1 \\ 0 \\ 0 \end{bmatrix} \tag{19}$$

is the Jacobian of the indicator function h and

$$\mathbf{G}(\mathbf{z}_-) = \mathbf{G}(\mathbf{z}(\tau_{i+1}^-)) = \left.\frac{\partial \mathbf{g}(\mathbf{z})}{\partial \mathbf{z}^T}\right|_{\mathbf{z}=\mathbf{z}(\tau_{i+1}^-)} = \begin{bmatrix} 1 & 0 & 0 \\ 0 & e & 0 \\ 0 & 0 & 1 \end{bmatrix} \tag{20}$$

is the Jacobian of the transition condition $\mathbf{g}$. After the impact the linearized equations for $\tau > \tau_{i+1}$ follow from

$$\tau > \tau_{i+1} : \delta\mathbf{z}' = \mathbf{F}(\tau)\delta\mathbf{z}, \delta\mathbf{z}(\tau_{i+1}) = \delta\mathbf{z}_+. \tag{21}$$

Using now the Eqs. (17), (18) and (21) we can calculate the spectrum of Lyapunov exponents for the nonsmooth system of the impact oscillator by applying the algorithms of Benettin et al. [1980] or Wolf et al. [1985].

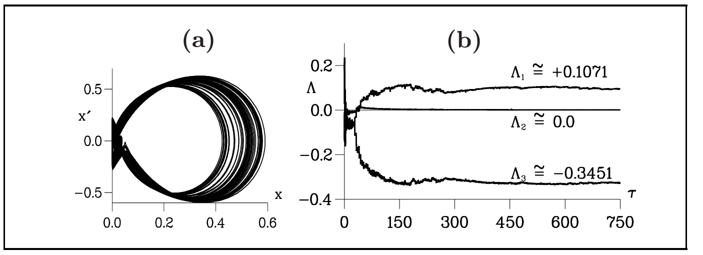

Figure 10. CONVERGENCE OF THE LYAPUNOV EXPONENTS ($D = 0.0, u_0 = 1.0, r = 0.8, \sigma = 0.0, \eta = 3.126$).

We now present some results of successful computations using this method. Figure 10(a) shows a chaotic solution for the impact oscillator in the (x, v) phase plane and Fig. 10(b) the convergence of the Lyapunov spectrum as $\tau \to \infty$. As the solution is chaotic, one Lyapunov exponent is positive, one equals zero corresponding to the tangential perturbation direction and one is negative. Figure 11 shows a bifurcation diagram for the impact oscillator and the corresponding Lyapunov exponents. On this diagram the location of a period doubling coincides with two Lyapunov exponents equaling zero. Using the results of the previous section we can now determine a relation between the nonzero Lyapunov exponents. The average rate of contraction for a set of area A in the (x, v) phase space over the time interval $T = 2\pi/\eta$ is given by

$$Ae^{(\Lambda_1+\Lambda_2)2\pi/\eta},$$

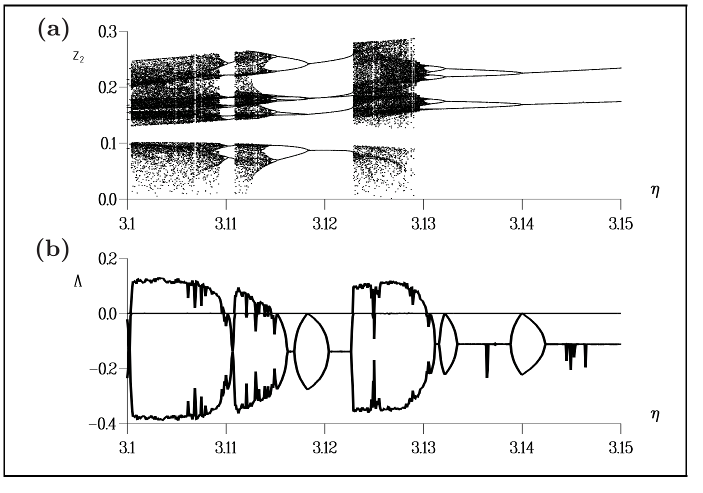

Figure 11. BIFURCATION DIAGRAM AND THE CORRESPONDING LYAPUNOV EXPONENTS ($D = 0.0, u_0 = 1.0, r = 0.8, \sigma = 0.0$).

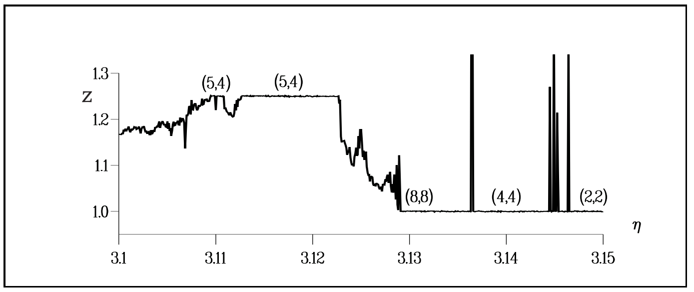

Figure 12. WINDING NUMBER FOR THE IMPACT OSCILLATOR, CP. WITH FIG. 11 ($D = 0.0, u_0 = 1.0, r = 0.8, \sigma = 0.0$).

however from (13,14) we also have that this rate of contraction is given by Ar^{2z}. Equating we have

$$\Lambda_1 + \Lambda_3 = \frac{\eta}{\pi} z \log(r). \tag{22}$$

hence the winding number and the Lyapunov exponents are closely related. Note that if Λ_1 and Λ_2 are both complex then we have

$$Re(\Lambda_1) = \frac{\eta}{2\pi} z \log(r)$$

which is approximately constant if η varies slowly. This observation accounts for some of the behaviour of the Lyapunov exponents visible in the figure. To confirm this relation we take the previous graph of the Lyapunov exponents and use equation (22) to estimate z. At the same time we calculate z directly from the flow. The two results are superimposed on Figure 12 and show close agreement.

Several interesting properties of the dynamics can be deduced from this picture. Note that the winding number remains constant during an orbit and through the period doubling bifurcations of that orbit. Further note the non rational values taken on the chaotic orbits.

CONCLUSION

This paper deals with a nonsmooth impact oscillator. The investigation of nonsmooth dynamical systems is presently a challenge for dynamisists and mathematicians, because many well known algorithms based on smoothness assumptions cannot be applied for systems with discontinuities. In this investigation the dynamical behaviour of an impact oscillator has been determined by experiments and compared to simulations. The application of Newton's impact law led to a good agreement of measured and simulated phase curves, bifurcation diagrams and Poincaré-maps. The higher mode oscillations and the deformations during the impacts do not affect the qualitative behaviour and the periodicity of the solution. Therefore, in the present paper analytical and model based methods for the analysis of the impact oscillator have been investigated. To gain insight into the system behaviour, the calculation of Lyapunov exponents and an analysis with the help of a two-dimensional impact map have been done. An analytic expression for the sum of Lyapunov exponents is found and used for the determination of the winding number.

REFERENCES

diBernardo, M.; Fossas, E.; Olivar, G.; Vasca, F., 1996, "Secondary bifurcations and high periodic orbits in a voltage controlled buck convertor", Applied Nonlinear Mathematics Report, University of Bristol, 14

Benettin, G.; Galgani, L.; Giorgilli, A.; Strelcyn, J.M., 1980, "Lyaponuov characteristic exponents for smooth dynamical systems and for Hamiltonian systems; a method for computing all of them", Meccanica, 15, No. 9, pp. 9-30

Budd, C.; Dux, F., 1994a, "Chattering and related behaviour in impact oscillators", Phil. Trans. R. Soc. Lond. A, 347, pp. 365-389

Budd, C.; Dux, F., 1994b, "Intermittency in impact oscillators close to resonance", Nonlinearity, 7, pp. 1191-1224

Budd, C., 1995a, "The global behaviour of impacting oscillators", Real and Complex Dynamical Systems, Kluwer Academic

Budd, C., 1995b, "Grazing in impact oscillators", Real and Complex Dynamical Systems, Kluwer Academic

Budd, C.; Dux, F.; Cliffe, A., 1995c, "The effect of frequency and clearance variations on single-degree-of-freedom impact oscillators", J. of Sound and Vibration, 184, No. 3, pp. 475-502

Budd, C., 1996a, "Non-smooth dynamical systems and the grazing bifurcation", In: Nonlinear Mathematics and Applications, P.Aston (Ed.), Cambridge University Press, pp. 219-235

Budd, C.; Lee, A.G., 1996b, "Double impact orbits of periodically forced impact oscillators", Proc. R. Soc. Lond. A, 452, pp. 2719-2750

Foale, S.; Bishop, S.R., 1992, "Dynamical complexities of forced impacting systems", Phil. Trans. R. Soc. Lond. A, 338, pp. 547-556

Chin, W.; Ott, E.; Nusse, H.; Grebogi, C., 1994, "Grazing bifurcations in impact oscillators", Phys. Rev. E, 50, pp. 4427-4444

Hinrichs, N.; Oestreich, M; Popp, K., 1997a, "Dynamics of oscillators with impact and friction", Chaos, Solitons &

Fractals, 8, No. 4, Special issue: Nonlinearities in applied engineering systems, pp. 535-558

Hinrichs, N.; Oestreich, M; Popp, K., 1997b, "Friction induced vibrations: Experiments, Modelling and Analysis", ASME: Dynamics of Systems with Friction and Impacts, Sacramento

Hubbuch, F.; Kunze, M.; Küpper, T., 1995, "Lyapunov exponents and qualitative analysis of some non-smooth dynamical systems", Dynamik: Analysis, effiziente Simulation und Ergodentheorie, Preprint, 24

Kaharaman, A.; Singh, R., 1990, "Nonlinear dynamics of a spur gear pair", J. of Sound and Vibration, 142, No. 1, pp. 49-75

Lamba, H.; Budd,C., 1994, "Scaling of Lyapunov exponents at non-smooth bifurcations", Phys. Rev E, 20, pp. 84-91.

McGeer, T., 1990, "Passive dynamic walking", Int. J. of Robotics Research, 9, pp. 62-82.

Müller, A; Hubbuch, F., 1995, "Lyapunov Exponenten in nicht-glatten Systemen", ZAMM: Z. angew. Math. Mech, 75, SI, T91-T92

Müller, P.C., 1995, "Calculation of Ljapunov exponents for dynamic systems with discontinuities", Chaos, Solitons & Fractals, 5, No. 9, pp. 1671-1681

Nordmark, A.B., 1991, "Non-periodic motion caused by grazing incidence in an impact oscillator", J. of Sound and Vibration, 145, No. 2, pp. 279-297

Oestreich, M.; Hinrichs, N.; Popp, K., 1996a, "Bifurcation and stability analysis for a non-smooth friction oscillator", Arch. Appl. Mech., 66, No. 5, pp. 301-314

Oestreich, M.; Hinrichs, N.; Popp, K., 1996b, "Signal and model based analysis of systems with friction and impact", IMECE: Elasto-Impact and Friction in Dynamic Systems, Atlanta, pp. 1-8

Peterka, F., 1974a, "Theoretical analysis of n-multiple (1/n)-impact solutions", Part 1, CSAV Acta Technica, 19, No. 4, pp. 462-473

Peterka, F., 1974b, "Results of analogue computer modelling of the motion", Part 2, CSAV Acta Technica, 19, No. 5, pp. 569-580

Popp, K.; Hinrichs, N; Oestreich, M., 1995, "Dynamical behaviour of a friction oscillator with simultaneous self and external excitation", Sãdhanã, 20, Part. 2-4, pp. 627-654

Popp, K.; Hinrichs, N; Oestreich, M., 1996, "Analysis of a self excited friction oscillator with external excitation", In: Guran, A; Pfeiffer, F; Popp, K. (Eds.), Dynamics with friction: Modeling, Analysis and Experiment, World Scientific, pp. 1-35

Prestl, W., 1990, "Zahnhämmern in Rädertrieben von Dieselmotoren", München, Technische Universität, Diss., -Fortschr.-Ber. VDI Reihe 11, Nr. 145. Düsseldorf: VDI-Verlag

Shaw, S.W.; Holmes, P.J., 1983, "Periodically forced linear oscillator with impacts: Chaos and long-period motions", Phys. Review Letters, 51, No. 8, pp. 623-626

Stensson, A.; Nordmark, A.B., 1994, "Experimental investigation of some consequences of low velocity impacts in the chaotic dynamics of a mechanical system", Phil. Trans. R. Soc. Lond. A, 347, pp. 439-448

Tung, P.C.; Shaw, S.W., 1988, "A method for the improvement of impact printer performance", Trans. ASME: J. of Vib., Acoustics, Stress, and Reliability in Design, 110, pp. 528-532

Whiston,G.S., 1987, "The vibro-impact response of a harmonically excited and preloaded impact oscillator", J. Sound and Vibration, 115, pp. 303-324

Wolf, A.; Swift, J.; Swinney, H.; Vastano, J., 1985, "Determining Lyapunov exponents from a time series", Physica D, 16, pp. 285-317